Functional Expression and Characterization of a Voltage-Gated $Ca_V1.3$ (α_{1D}) Calcium Channel Subunit from an Insulin-Secreting Cell Line

Alexandra Scholze, Tim D. Plant, Annette C. Dolphin, and Bernd Nürnberg

Institut für Pharmakologie (A.S., T.D.P., B.N.)
Freie Universität Berlin
14195 Berlin, Germany

Department of Pharmacology
University College London (A.C.D.)
WC1E 6BT, United Kingdom

Abteilung für Pharmakologie und Toxikologie (B.N.)
Universität Ulm
89081 Ulm, Germany

L-type calcium channels mediate depolarization-induced calcium influx in insulin-secreting cells and are thought to be modulated by G protein-coupled receptors (GPCRs). The major fraction of L-type α_1-subunits in pancreatic β-cells is of the neuroendocrine subtype ($Ca_V1.3$ or α_{1D}). Here we studied the biophysical properties and receptor regulation of a $Ca_V1.3$ subunit previously cloned from HIT-T15 cells. In doing so, we compared this neuroendocrine $Ca_V1.3$ channel with the cardiac L-type channel $Ca_V1.2a$ (or $\alpha_{1C\text{-}a}$) after expression together with $\alpha_2\delta$- and β_3-subunits in *Xenopus* oocytes. Both the current voltage relation and voltage dependence of inactivation for the neuroendocrine $Ca_V1.3$ channel were shifted to more negative potentials compared with the cardiac $Ca_V1.2$ channel. In addition, the $Ca_V1.3$ channel activated and inactivated more rapidly than the $Ca_V1.2a$ channel. Both subtypes showed a similar sensitivity to the dihydropyridine (+)isradipine. More interestingly, the $Ca_V1.3$ channels were found to be stimulated by ligand-bound G_i/G_o-coupled GPCRs whereas a neuronal $Ca_V2.2$ (or α_{1B}) channel was inhibited. The observed receptor-induced stimulation of $Ca_V1.3$ channels could be mimicked by phorbol-12-myristate-13-acetate and was sensitive to inhibitors of protein kinases, but not to the phosphoinositol-3-kinase-inhibitor wortmannin, pointing to serine/threonine kinase-dependent regulation. Taken together, we describe a neuroendocrine L-type $Ca_V1.3$ calcium channel that is stimulated by G_i/G_o-coupled GPCRs and differs significantly in distinct biophysical characteristics from the cardiac subtype ($Ca_V1.2a$), suggesting that the channels have different roles in native cells. (Molecular Endocrinology 15: 1211–1221, 2001)

0888-8809/01/$3.00/0
Molecular Endocrinology 15(7): 1211–1221

INTRODUCTION

Voltage-dependent calcium channels play a central role in the regulation of insulin secretion by pancreatic β-cells. However, the subtypes of calcium channels involved, their particular contribution to the secretion process, and their regulation by glucose and by transmitter substances are still controversial points. This is due, in part, to the fact that studies have been performed on native β-cells from different species and also on various insulin-secreting cell lines, *e.g.* HIT-cells and RINm5F cells.

Using molecular biological approaches, various pore-forming calcium channel α_1-subunits ($Ca_V1.2$, $Ca_V1.3$, $Ca_V2.1$, $Ca_V2.2$, $Ca_V2.3$, and $Ca_V3.1$) have been identified in insulin-secreting cells and pancreatic tissue (1–5). In electrophysiological studies, channel currents with the pharmacological and functional properties known for these subunits have also been reported. Thus, high-voltage-activated (HVA), dihydropyridine (DHP)-sensitive channels (6), corresponding to the $Ca_V1.2$ or $Ca_V1.3$ subunits, ω-conotoxin GVIA-sensitive channels (7, 8), corresponding to the $Ca_V2.2$ subunit, and ω-agatoxin IVA-sensitive channels (5), corresponding to the $Ca_V2.1$ subunit, have been de-

scribed. Low-voltage-activated currents, which would correspond to the $Ca_V3.1$ subunit that has been found in the INS-1 cell line, have also been observed in several insulin-secreting cell types (4).

Taken together, insulin-secreting cells express multiple voltage-gated calcium channel subtypes, making it difficult to clarify the properties of a certain channel type in these cells. A common approach to address this problem is the use of cellular systems overexpressing the proteins of interest. This approach has already been extensively used to study the properties of channels formed by most of the calcium channel α_1-subunits [*e.g.* $Ca_V1.2$ (9, 10), $Ca_V2.1$ (11), $Ca_V2.2$ (9, 12, 13), $Ca_V2.3$ (11, 14); $Ca_V3.1$ (15, 16)].

In the case of the $Ca_V1.3$ subunit, however, which is thought to play a major role in the regulation of insulin secretion, few data are available (17, 18), although several splice variants were cloned (17–20). This subunit, in combination with the auxiliary subunits $\alpha_2\delta$ and β, forms an HVA-calcium channel of the L-type (for review see Refs. 21–23). Its occurrence is not restricted to the pancreas. Isoforms of the $Ca_V1.3$ subunit have been identified by RT-PCR, antibodies, or Northern blot analysis in brain, heart, kidney, adrenal gland, and osteoblasts (24–26). $Ca_V1.3$ is thought to comprise the major fraction of L-type calcium current in neurosecretory and neuronal cells (Refs. 22 and 27 but see also Ref. 25).

In pancreatic β-cells the majority of L-type calcium channel mRNA codes for $Ca_V1.3$ subunits (2, 28). So far, there is only a single brief report on the functional expression of a $Ca_V1.3$ channel cloned from an insulin secreting cell line [RINm5F (17)]. Hence, data on the functional properties and regulation of these neuroendocrine $Ca_V1.3$-derived pore-forming calcium channel subunits are still lacking. This prompted us to study the $Ca_V1.3$ isoform cloned from the insulin-secreting HIT-T15 cell line (19), after coexpression with the $\alpha_2\delta$ and β_3 subunits in *Xenopus* oocytes. Here, we provide the first description of the biophysical properties of this isoform and the first description of receptor regulation of a heterologously expressed pancreatic $Ca_V1.3$ channel.

RESULTS

Calcium Channel Expression

To examine the functional properties of calcium channels, we injected α_1 subunits encoding the neuroendocrine ($Ca_V1.3$), cardiac ($Ca_V1.2a$), or neuronal ($Ca_V2.2$) calcium channel together with the $\alpha_2\delta$ and β_3 subunits into oocytes. The resulting Ba^{2+} inward current amplitudes in subsequent voltage-clamp measurements were highly variable (Fig. 1A). Differences were considerable between individual donor toads, but much less within a batch of oocytes from the same animal. Uninjected oocytes showed either no detectable native calcium channel current, or inward currents with amplitudes of up to 50 nA. In oocyte batches from most donor animals, endogenous oocyte calcium channel currents were enhanced by exogenous $\alpha_2\delta$ and β subunits, as described previously (29). The resulting currents were often of considerable amplitude (see Fig. 1A), in agreement with one previous study (29), but in contrast to others (18, 30). Hereafter, the $\beta/\alpha_2\delta$-stimulated endogenous oocyte calcium channel is referred to as the endogenous calcium channel. To assess the effects on endogenous channels, all types of experiments on inward Ba^{2+} currents were also performed in cells injected with cRNA for the $\alpha_2\delta$ and β subunits. To minimize the contribution of currents through the endogenous channel, the amplitudes of currents through these channels were compared with those from cells injected with cRNA for the respective complete exogenous channel. Only those oocyte batches were used, in which a very large relative proportion (at least 80%) of total current was contributed by the exogenous channel subtype. Up to 20% of endogenous current was present in some cases when examining the $Ca_V1.3$ channel, since the amplitude of currents in oocytes expressing this channel was in general smaller than that in those expressing the cardiac $Ca_V1.2a$ or neuronal $Ca_V2.2$ subunits (compare Fig. 1A). These latter two α_1 subunits produced large currents, which were usually measurable on the second day after cRNA injection. In contrast, expression of the neuroendocrine $Ca_V1.3$ calcium channel exceeded expression of the endogenous channel to a sufficient extent for measurement only after 4–6 days.

When expressed without the auxiliary subunits $\alpha_2\delta$ and β ($n = 8$), the neuroendocrine $Ca_V1.3$ subunit did not produce inward currents exceeding those of noninjected oocytes, in contrast to the $Ca_V1.2a$ subunit (our unpublished data and Ref. 31). Currents of larger amplitude than those in control cells were also not observed when only $\alpha_2\delta$ was expressed together with $Ca_V1.3$. In contrast, when the β_3 subunit was coexpressed with $Ca_V1.3$ without $\alpha_2\delta$, the resulting current amplitudes were 22–50% of the corresponding $Ca_V1.3/\beta_3/\alpha_2\delta$ currents. In one batch of oocytes that did not display measurable endogenous calcium channel currents after injection of exogenous auxiliary subunits, the following maximum inward current amplitudes were obtained: $Ca_V1.3$: 0 nA ($n = 4$), $Ca_V1.3/\beta_3$: -152 ± 29 nA ($n = 6$), $Ca_V1.3/\beta_3/\alpha_2\delta$: -586 ± 141 nA ($n = 6$).

Activation of Ba^{2+} Currents

Analysis of the current-voltage (I-V) relationships for the neuroendocrine $Ca_V1.3$ and the cardiac $Ca_V1.2a$ channels (Fig. 1B) revealed significant differences with respect to the half-maximal activation parameters ($V_{1/2}$; $P < 0.05$), which were -9.6 ± 1.2 mV ($n = 17$) and -6.1 ± 1.2 mV ($n = 17$), but not for the slope factors (k), which were 7.5 ± 0.2 mV and 7.3 ± 0.4 mV, respectively. The maximum inward current for the neu-

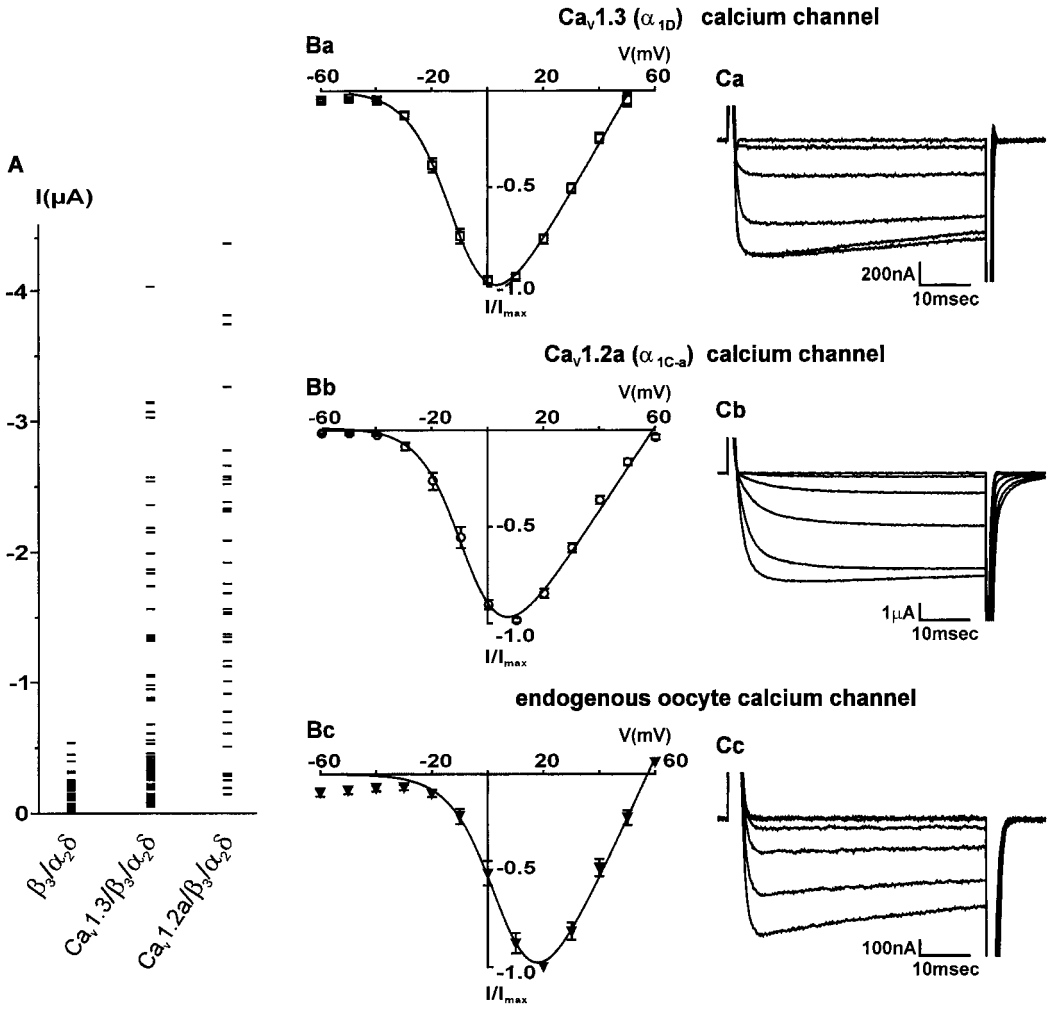

Fig. 1. Current Amplitudes, Average I-V Relationship, and Trace Examples of the Channels Examined

A, Maximum current amplitudes for endogenous oocyte (n = 69), the neuroendocrine $Ca_V1.3$ (n = 74), and the cardiac $Ca_V1.2a$ (n = 38) calcium channel current from six donor frogs. B, The average I-V relationship for a) the neuroendocrine $Ca_V1.3$ (n = 17), b) the cardiac $Ca_V1.2a$ (n = 17), and c) the endogenous oocyte (n = 14) calcium channel. Individual I-V curves were normalized to the maximum current, averaged, and then fitted with equation 1 yielding $V_{1/2} = -9.8$ mV for panel Ba, −6.7 mV for panel Bb, and 7.0 mV for panel Bc, respectively. C, In each case representative traces from voltage steps to −30, −20, −10, 0, 10, and 20 mV are shown. The examples in panels Ca–Cc correspond to panel B.

roendocrine $Ca_V1.3$ channel occurred at more negative potentials (2.7 ± 1.1 mV; n = 14) than for the cardiac $Ca_V1.2a$ channel (6.4 ± 1.1 mV; $P < 0.05$). The I-V relation of the endogenous calcium channel showed a $V_{1/2}$ that was significantly ($P < 0.001$) shifted to depolarized potentials compared with the $Ca_V1.3$ and the $Ca_V1.2a$ channels. Half-maximal activation occurred at 9.4 ± 1.1 mV, and the slope factor (k) was estimated to be 7.5 ± 0.4 mV. The maximum inward current was at 18.8 ± 1.0 mV, a value comparable to those published previously (10, 18, 31).

It is obvious from the current traces in Fig. 1C that the activation of the cardiac $Ca_V1.2a$ channel is slower than that of the neuroendocrine $Ca_V1.3$ or endogenous counterparts. The rising phase of currents elicited by depolarizing voltage steps was quantified by determining the time necessary to reach 90% of peak current [90% time-to-peak (ttp)] in each case (Fig. 2A). The cardiac $Ca_V1.2a$ calcium channel showed a significantly ($P < 0.05$) slower activation compared with the neuroendocrine $Ca_V1.3$ and the endogenous channel over the voltage range between −10 and +20 mV. The activation times for the neuroendocrine $Ca_V1.3$ and the endogenous oocyte channels were only significantly different ($P < 0.05$) at −10 mV. In addition, a voltage dependence of the values for 90% ttp was observed for all three channels with values decreasing with increasing depolarization. This decrease with potential was, however, only significant ($P < 0.05$) for the neuroendocrine $Ca_V1.3$ and the cardiac $Ca_V1.2a$ channels, when the values of 90% ttp at the different voltages were compared for each individual subtype.

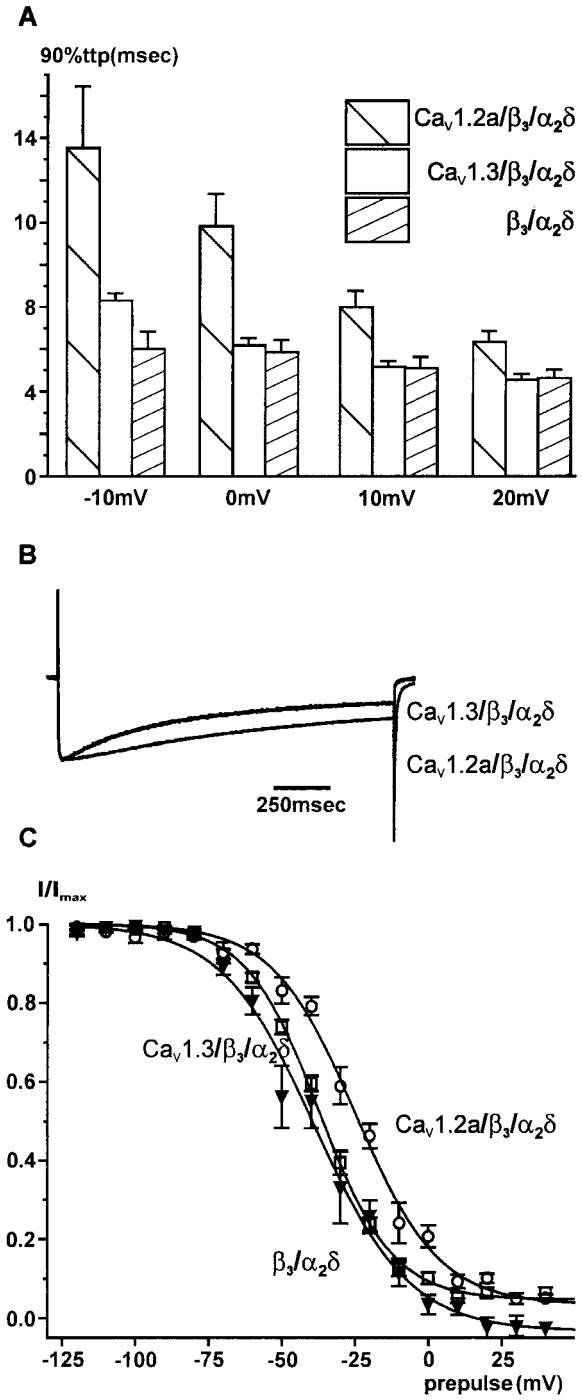

Fig. 2. Time Dependence of Calcium Channel Activation, Current Decay, and Steady-State Inactivation

A, Time-to-90% peak current (90% ttp) during voltage pulses to the indicated potentials for the neuroendocrine $Ca_V1.3$ (n = 5), the cardiac $Ca_V1.2a$ (n = 5), and the endogenous oocyte (n = 5) calcium channel. B, Channel inactivation during 1,500 msec voltage steps to the maximum of the individual I-V curve. Traces were normalized to the maximum current and a representative example is shown for each case. C, Steady-state inactivation data were deduced from peak currents at 0 mV reached after a prepulse to the indicated potentials. Data were pooled from experiments with prepulse lengths between 10 and 90 sec; no significant differences were observed between the differing protocols. The prepulse and the test pulse were separated by a 10- to 20-msec interval at −80 mV. Individual inactivation curves were normalized to the maximum current, averaged, and fitted, yielding a half-maximal inactivation at −37.1 mV for the $Ca_V1.3$ (□; n = 24), −24.7 mV for the cardiac $Ca_V1.2a$ (○; n = 20), and −38.5 mV for the endogenous (▼; n = 7) calcium channel.

Inactivation of Ba^{2+} Currents

From the current traces in Figs. 1C and 2B, it is clear that the rate of inactivation of calcium channel currents differs for the neuroendocrine $Ca_V1.3$, cardiac $Ca_V1.2a$, and endogenous channel subtypes. When the current decay during longer depolarizing voltage steps was analyzed in detail, it was found to be best fitted by a monoexponential function (eq 4) when pulses of 1,500 msec were used. Currents during longer pulses (5 sec) were better fitted by a biexponential function (eq 5, values in Table 1). The neuroendocrine $Ca_V1.3$ and the cardiac $Ca_V1.2a$ channels differed significantly, both in their τ_1 ($P < 0.005$) and τ_2 ($P < 0.005$) values and in the ratio of the amplitudes of the fast and the slow current components (A_1/A_2, $P < 0.001$). The endogenous channel inactivated most rapidly, but differed significantly ($P < 0.05$) from the neuroendocrine $Ca_V1.3$ channel only in the τ_1 value for the fast current component.

Comparing fits of a monoexponential function to currents during 1,500-msec pulses to the maximum of the individual I-V curve (see Fig. 2B), τ was 546 ± 23 msec (n = 17) for the neuroendocrine $Ca_V1.3$ and 972 ± 126 msec (n = 9) for the cardiac $Ca_V1.2a$ calcium channel, values that were significantly different ($P < 0.001$; see also Fig. 2B). Since endogenous oocyte Ca^{2+}-activated Cl^- conductances may obscure the measurement of inactivation of calcium channels, additional experiments were performed on oocytes with the calcium chelator BAPTA [1,2-bis(o-amino-5-bromophenoxy)ethane-*N*,*N*,*N*′,*N*′-tetraacetic acid, sodium] present inside the cell. The currents during 1,500-msec pulses to the maximum of the individual I-V curve fitted with a monoexponential function, τ was 530 ± 15 msec (n = 26) for the neuroendocrine $Ca_V1.3$ and 966 ± 88 msec (n = 14) for the cardiac $Ca_V1.2a$ calcium channel, values that were significantly different ($P < 0.001$). Hence, the rate of inactivation of $Ca_V1.2a$ channels was significantly different from inactivation of $Ca_V1.3$ channels, both in the presence and absence of the intracellular Ca^{2+} chelator BAPTA.

Potential Dependence of Ba^{2+} Current Inactivation

The steady-state inactivation was measured with a two-step protocol. The inactivation curves are shown

Table 1. Values from Biexponential Fitting of Current Decay in Calcium Channels

Subunit Combination	τ_1 (msec)	τ_2 (msec)	A_1/A_2
$Ca_V1.3 + \beta_3 + \alpha_2/\delta$	259 ± 16	1,500 ± 73	1.7 ± 0.2
$Ca_V1.2a + \beta_3 + \alpha_2/\delta$	520 ± 73	2,814 ± 307	0.5 ± 0.1
$\beta_3 + \alpha_2/\delta$	147 ± 33	1,499 ± 372	2.1 ± 0.5

Currents with a duration of 5 sec derived from voltage steps to the potential of peak current amplitude in the individual I-V curves could be best fitted by a biexponential function, resulting in a fast (τ_1) and a slow (τ_2) inactivating component. The term A_1/A_2 gives the relation between the maximal current amplitudes of the components. For the neuroendocrine $Ca_V1.3$ channel: n = 5; cardiac $Ca_V1.2a$: n = 5; endogenous: n = 5.

in Fig. 2C. Their analysis indicated that the cardiac $Ca_V1.2a$ and the neuroendocrine $Ca_V1.3$ channels differ significantly ($P < 0.001$) in their half-maximal inactivation, with respective $V_{1/2}$ values of −22.7 ± 1.7 (n = 20) and −36.1 ± 0.9 mV (n = 24). Values for the endogenous calcium channel ($V_{1/2}$ = −35.0 ± 3.5 mV; n = 7) differed significantly from both other channels ($P = 0.001$). The slope factor (k) was almost identical for all three channels (neuroendocrine $Ca_V1.3$: 12.7 ± 0.3 mV; cardiac $Ca_V1.2a$: 14.0 ± 0.7 mV; and endogenous: 14.4 ± 1.2 mV).

In addition, we analyzed steady-state inactivation in the presence of intracellular BAPTA. The results also showed a significant difference ($P < 0.001$) between the cardiac $Ca_V1.2a$ channel ($V_{1/2}$ = −20.5 ± 2.3 mV; n = 15) and the neuroendocrine $Ca_V1.3$ channel ($V_{1/2}$ = −30.9 ± 1.2 mV; n = 17).

Current Characterization by Blocking Agents

HVA calcium currents in native β-cells have been shown to be blocked completely by 200 μM Cd^{2+} (8). Addition of 200 μM Cd^{2+} to the bath solution abolished currents through the $Ca_V1.3/\beta_3/\alpha_2\delta$ (n = 6) as well as the $Ca_V1.2a/\beta_3/\alpha_2\delta$ (n = 4) calcium channels.

An important distinguishing feature for L-type calcium channels is their sensitivity to DHPs. We therefore compared the DHP sensitivity of the neuroendocrine $Ca_V1.3$, cardiac $Ca_V1.2a$, and endogenous channels. Using (+)isradipine (Fig. 3), we found a 50% inhibition of the DHP-sensitive fraction of the current at a concentration of 43 nM for the cardiac $Ca_V1.2a$ channel and a similar value of 57 nM for the neuroendocrine $Ca_V1.3$ channel. The endogenous current was not inhibited by (+)isradipine at concentrations up to 3 μM (n = 7), as also shown in other studies (31, 32).

Regulation of the Expressed Calcium Channels

Previously, we and others have found a G protein-dependent inhibition of L-type calcium channels in neuroendocrine cells (7, 33, 34) resembling membrane-delimited inhibition of calcium channel $\alpha_{1A,B,E}$-

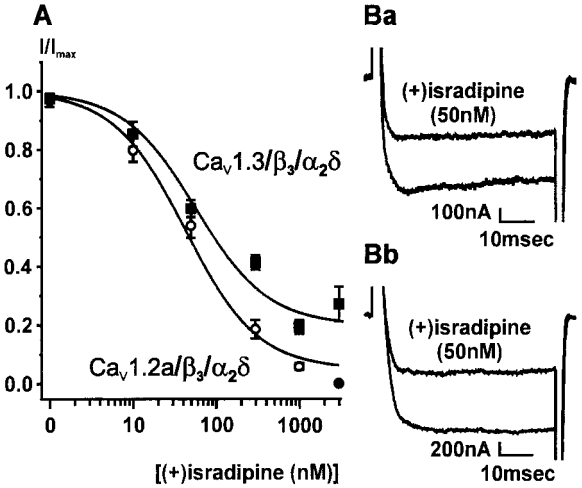

Fig. 3. Comparison of Dihydropyridine Sensitivity of Calcium Channels Composed of $Ca_V1.3$ and $Ca_V1.2a$ Subunits

A, Peak currents within a 50-msec test pulse to 0 mV and an interpulse interval of 30 sec were measured. The (+)isradipine stock was diluted in the bath solution to the indicated concentrations and applied. Data points are quotients of the current amplitude before (+)isradipine application and the point of maximal inhibition (n = 3–5 for each point). Curve fitting (eq 6) revealed an IC_{50} of 57 nM for the $Ca_V1.3$ (■) and 43 nM for the cardiac $Ca_V1.2a$ (○) calcium channel. B, Example of isradipine inhibition for both channels close to the IC_{50} (neuroendocrine $Ca_V1.3$, Ba; cardiac $Ca_V1.2a$, Bb). A control trace and one of maximal inhibition during isradipine application are shown for each case.

subunits by Gβγ-complexes (12, 35, 36). Furthermore, the neuroendocrine $Ca_V1.3$ calcium channel subtype, in particular, has been proposed to be affected by this inhibition (for review see Ref. 22). This prompted us to examine the regulation of the neuroendocrine $Ca_V1.3$ channel from HIT-T15 cells in oocytes coinjected with the G_i/G_o-coupled μ-opioid receptor. In our hands, this receptor was able to couple to endogenous phospholipase C in oocytes, as indicated by the stimulation of calcium-dependent chloride currents (n = 14) after receptor activation with the selective μ-opioid receptor agonist DAMGO ([D-Ala^2,*N*-Me-Phe^4,Gly-ol^5]-enkephalin) in oocytes bathed in modified Ringer. Furthermore, we have ascertained that the μ-opioid receptor used in this study couples only to pertussis toxin-sensitive G proteins of the G_i-subfamily regardless of which agonist was used (37). Moreover, as a control for G protein-mediated inhibition in this system, we tested the neuronal (N-type) $Ca_V2.2$ (or α_{1B}) calcium channel. This channel is the classical example of a voltage-dependent calcium channel inhibited by PT-sensitive G proteins (38, 39). As depicted in Fig. 4, application of DAMGO to oocytes coexpressing μ-opioid receptors and $Ca_V2.2$ channels resulted in a rapid inhibition of inward currents. The concentration of DAMGO necessary to maximally inhibit this channel was determined from the dose-response relation, which revealed an IC_{50} of

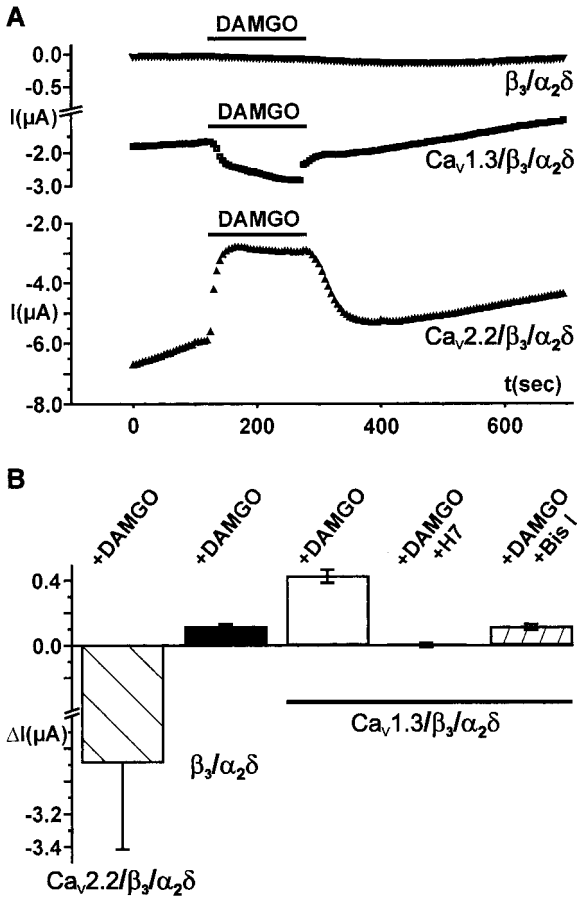

Fig. 4. Channel Regulation via the μ-Opioid Receptor Agonist DAMGO (1 μM)

A, Typical current amplitude measurements representing peak currents at voltage steps to 0 mV are shown for the $Ca_V1.3$ (□), the endogenous oocyte (▼), and the neuronal (▲) calcium channel. The pulse frequency was 0.2 Hz. B, Maximum current changes under DAMGO application (2.5 min) for the neuronal (n = 7), the endogenous (n = 23), and the neuroendocrine $Ca_V1.3$ (n = 26) calcium channel. The fourth column shows the DAMGO effect on the neuroendocrine $Ca_V1.3$ channel after preincubation with H7 (100 μM; n = 5); the fifth column shows the DAMGO effect on this channel after preincubation with bisindolylmaleimide I (Bis I; 100 nM; n = 5). Both inhibitors were also present during the DAMGO application in the respective experiments.

1.1 nM and maximal inhibition with concentrations above 100 nM (n = 3–5). This maximal inhibition was approximately 60%, in accordance with previous studies of this channel when expressed with calcium channel β subunits (9, 40). In contrast to the neuronal $Ca_V2.2$, the neuroendocrine $Ca_V1.3$ channel was stimulated by DAMGO at a maximally effective concentration (1 μM). The effect started within a few seconds of agonist application, reached a maximum increase of 406 ± 49 nA (28 ± 2%, n = 20) within 2 min, and was reversible upon washout of the agonist (see Fig. 4). To exclude nonspecific, receptor-independent effects, DAMGO was applied at the same concentration to cells injected with cRNA for the neuroendocrine $Ca_V1.3$ channel, but not for the μ-opioid receptor. No stimulation of inward current was observed (n = 5) under these conditions or after the application of bath solution without DAMGO to cells expressing the μ-opioid receptor and neuroendocrine $Ca_V1.3$ channel (n = 3). Since it was shown by Zamponi *et al.* (40) that G protein-mediated inhibition can be impaired as a result of channel phosphorylation by protein kinase C (PKC), oocytes were incubated with H7 at a high concentration (100 μM) to inhibit serine/threonine kinase-dependent phosphorylation as completely as possible (Fig. 4B). After 5 min (n = 3) or 30 min (n = 2) of preincubation with H7, the increase in current through the neuroendocrine $Ca_V1.3$ channel after opioid receptor activation was prevented. However, under these conditions DAMGO still failed to induce calcium channel inhibition (see Fig. 4B). We therefore concluded that DAMGO-induced neuroendocrine $Ca_V1.3$ calcium channel stimulation involved protein phosphorylation. Stimulation of calcium channel currents in neuroendocrine cells resulting from phosphorylation by protein kinase A (PKA) and PKC has been reported in several studies (41, 42). Since PKA can also be inhibited by H7 (43), we tested the effect of PKA inhibition on receptor-stimulated channel activity. The response of the neuroendocrine $Ca_V1.3$ calcium channel to receptor activation in oocytes injected with the PKA-inhibitor Rp-cAMPS (adenosine 3′,5′-cyclic phosphorothiolate-Rp) [to calculated final concentrations of 50 μM (n = 4) and 400 μM (n = 5), 15–20 min before experiments], did not significantly differ from that in control cells without Rp-cAMPS (n = 9). Since L-type calcium channels are known to be stimulated by G protein-coupled receptors (GPCRs) in a phosphoinositol-3-kinase (PI3K)- and/or PKC-dependent manner, we tested the effects of the PI3K-inhibitor wortmannin and the PKC-inhibitor bisindolylmaleimide I on calcium current stimulation. Incubation of oocytes with 150 nM and 500 nM wortmannin in the extracellular solution for 20 min did not result in a significant reduction of the DAMGO-induced effect (n = 5). In contrast, preincubation of oocytes with bisindolylmaleimide I (100 nM, 1 h) resulted in a significant reduction of DAMGO-induced calcium current stimulation ($P < 0.005$; Fig. 4B). Furthermore, we used the phorbol ester phorbol myristate acetate (PMA) to directly activate PKC and obviate potential complications due to overlapping inhibitory effects via $G_{i/o}$ proteins and stimulatory effects via PKC on calcium channel activity. In line with the results obtained with DAMGO, acute application of PMA (100 nM; n = 12) increased the Ba^{2+} inward current (107.5 ± 13.4 nA, n = 12) significantly within 2.5 min when compared with results from experiments with vehicle only (46.7 ± 11.1 nA, n = 9) in cells overexpressing the neuroendocrine $Ca_V1.3$ channel ($P < 0.005$).

It should be mentioned that the endogenous oocyte calcium channel was also stimulated by DAMGO. Even though this stimulation was pronounced (200 ± 21%), the absolute amplitude of the effect and the

kinetics of this stimulation allowed a clear distinction between the responses of the neuroendocrine $Ca_V1.3$ and the endogenous channel (see Fig. 4). After agonist application, the increase in currents through the endogenous channel started with a delay, reaching a maximum usually during washout of the agonist (see Fig. 4). Since no current stimulation occurred in the presence of H7, stimulation of the endogenous channel probably results from protein phosphorylation. This observation is also in agreement with those that showed that the amplitude of currents through the endogenous oocyte calcium channel was increased by PMA (Ref. 32 and our unpublished data).

DISCUSSION

Here we describe the successful expression of a previously cloned neuroendocrine L-type calcium channel consisting of the $Ca_V1.3$ subunit from insulin-secreting cells together with the β_3 and $\alpha_2\delta$ subunits (19). Channels of this subunit combination are likely to occur in native endocrine cells since $Ca_V1.3$, β_2, and β_3 have been found to coincide in RINm5F cells (17). Furthermore, studies using *in situ* hybridization and immunostaining found a colocalization of $Ca_V1.3$ and β_3 in several brain areas (44).

Notably, currents through this neuroendocrine channel were not observed upon expression of the $Ca_V1.3$ subunit alone or in combination with $\alpha_2\delta$. Hence, its association with at least β subunits seem to be essential for functional expression, as also reported for two other $Ca_V1.3$ isoforms (17, 18). Nevertheless, upon coexpression of $\alpha_2\delta$ with the $Ca_V1.3/\beta_3$ subunits, the amplitude of neuroendocrine $Ca_V1.3$ channel currents was increased by 2- to 5-fold in the present study. Similar effects of the $\alpha_2\delta$ subunit on the $Ca_V2.1/\beta$ combination were reported by de Waard and Campbell (30), who found a 2.5-fold current increase. An even more pronounced effect (~15-fold stimulation) was also reported (10), when $Ca_V1.2a/\beta/\alpha_2\delta$ channels were compared with $Ca_V1.2a/\beta$ channels.

The neuroendocrine $Ca_V1.3$ channel examined here yielded, on average, relatively low current amplitudes as compared with channels formed by the $Ca_V2.2$ and $Ca_V1.2a$ subunits in the same expression system. Furthermore, the time interval after cRNA injection that was necessary to obtain currents of sufficient amplitude for kinetic analysis was longer than that required for the other α_1 subunits. Reasons for this observation may be inherent to the $Ca_V1.3$ subunit itself. As suggested by Hofmann *et al.* (23), one reason may be the need for additional, possibly still unidentified, auxiliary subunits. Another possible cause could be the necessity for specific interactions with additional proteins, as described for syntaxin and the $Ca_V1.3a$ subunit in pancreatic β-cells (27).

When the I-V curves for the neuroendocrine $Ca_V1.3$ channel used in the present study were analyzed, the maximum inward currents were found to occur at potentials between 0 and +10 mV. A similar value of 0 mV was reported by Williams *et al.* (18) for a neuronal $Ca_V1.3/\beta_2/\alpha_2\delta$ subunit combination expressed in *Xenopus* oocytes. A particularly interesting native cell for comparison in this respect is the rat pinealocyte, which has been shown to contain $Ca_V1.3$ as the sole calcium channel α_1 subunit, together with the β_2 and β_4 subunits. The minimum of the I-V curve in these cells is also between 0 and 10 mV at similar Ba^{2+} concentrations (26). When comparing the potential dependence of the currents, it should be kept in mind that the β subunit type also influences this property of calcium channels and, thus, the position of the I-V curve (23). The comparison of the I-V minima, which we performed here, seems to be applicable, since at least in the case of the $Ca_V2.1$ subunit, β_2 or β_3, the isoform used in the present study, had a similar influence on the potential dependence of the currents (30).

During prolonged depolarizations, the neuroendocrine $Ca_V1.3$ channel showed slow inactivation with Ba^{2+} as the charge carrier. Inactivation was, however, on average twice as fast for the neuroendocrine $Ca_V1.3$ than for the cardiac $Ca_V1.2a$ channel. The voltage dependence of inactivation also differed significantly between these two L-type channels, with the neuroendocrine $Ca_V1.3$ subtype inactivating at more negative membrane potentials. In mouse pancreatic β-cells, where the majority of the calcium current has been reported to be DHP-sensitive, inactivation during short voltage pulses was shown to be almost purely Ca^{2+}-dependent (3). Other authors also reported a strong calcium-dependence in mouse pancreatic β-cells (45), but detected an additional slower voltage-dependent component of HVA current inactivation when using longer depolarizing pulses and Ba^{2+} as the charge carrier. The inactivation of the neuroendocrine $Ca_V1.3$ channel in our study, also using Ba^{2+} as the charge carrier, could partially reflect this component. Although the Ca^{2+}-dependent component dominates inactivation in β-cells, slower voltage-dependent inactivation could play a role in the regulation of calcium entry during slow wave depolarization.

Sensitivity to DHPs is a property that has frequently been used to distinguish the role of different calcium channel subtypes in the regulation of insulin secretion and the signal transduction processes in insulin-secreting cells (6, 46, 47). Comparison of the DHP sensitivity of the neuroendocrine $Ca_V1.3$ and the cardiac $Ca_V1.2a$ channel revealed similar IC_{50} values for (+)isradipine. Therefore, this DHP does not discriminate between these two channel isoforms.

Regulation of L-type calcium channels in insulin-secreting cells, either directly by heterotrimeric G proteins or through second messengers, is a matter of intense research (6, 42). For instance, GPCRs have been reported to inhibit L-type calcium currents in insulin-secreting RINm5F cells via PT-sensitive G proteins (6, 7, 47). Since heterologously expressed $Ca_V1.2$ (α_{1C}) calcium channels are not a target for G

protein-dependent inhibition (9, 35), $Ca_V1.3$ (α_{1D}) isoforms are L-type channel candidates for inhibition by G proteins. However, in the present study, activation of PT-sensitive G proteins by μ-opioid receptors did not result in inhibition of the neuroendocrine calcium channel ($Ca_V1.3$ or α_{1D}) despite clear inhibition of the neuronal calcium channel ($Ca_V2.2$ or α_{1B}) under identical experimental conditions. In this context it should be noted that the $Ca_V2.2$ contains the known G$\beta\gamma$-binding motif QXXER present in the intracellular loop between repeats I and II. Resequencing of the $Ca_V1.3$ by us revealed the presence of a QXXEE-amino acid motif in the loop I-II sequence, which has been found in various L-type calcium channels including a neuronal isoform known not to be directly inhibited by G$\beta\gamma$ (23, 39, 48).

In contrast, we found that currents through this $Ca_V1.3$ channel were increased after receptor activation. The stimulation of the $Ca_V1.3$ channel is clearly distinguishable from that of the endogenous channel both in time course and amplitude. The finding that the specific kinase inhibitors H7 and bisindolylmaleimide I abolished this receptor-induced current stimulation is mechanistically relevant and points to the involvement of a kinase. Stimulation of voltage-dependent calcium channels by PKC or PKA is well established (23). H7 inhibits both kinases with IC_{50} values in a comparable range whereas bisindolylmaleimide I is a potent inhibitor of PKC (43, 49). Furthermore, we recently showed that smooth muscle L-type calcium channels are activated by G$\beta\gamma$-subunits via PKC- and PI3K-dependent pathways (50, 51). However, for GPCR-controlled regulation of the $Ca_V1.3$ channel examined in this study, the involvement of PI3K is unlikely, since the specific PI3K inhibitor wortmannin did not affect receptor-induced stimulation of the $Ca_V1.3$ channel at a concentration known to block class I PI3Ks (data not shown). Also, the involvement of PKA in transmitting the stimulatory activity from the receptor to the $Ca_V1.3$ channel is unlikely based on independent and complementary experimental approaches. First, we ascertained that the human μ-opioid receptor used in the present study couples exclusively to members of the G_i/G_o family but not to G_s proteins, which are upstream activators of adenylyl cyclases and PKA (37). This selective coupling between the receptor and G proteins was independent of the ligand used. Second, a stimulation by the downstream effector PKA was ruled out by using the PKA inhibitor Rp-cAMPS. In contrast, several considerations argue for an involvement of PKC in stimulation of the $Ca_V1.3$ channel by the G_i/G_o-coupled μ-opioid receptor. It is well documented that PKC is activated by PT-sensitive GPCRs via G_i/G_o proteins and phospholipase C (for review see Ref. 52). Accordingly, we confirmed that the μ-opioid receptor expressed in *Xenopus* oocytes was able to activate a calcium-dependent chloride current under appropriate experimental conditions. This stimulatory effect in *Xenopus* oocytes is an established read-out system to detect coupling between receptors and endogenous phospholipase C, the key regulator of PKC (53). We also confirmed in a more direct fashion the ability of PKC to stimulate the $Ca_V1.3$ channel using the PKC activator PMA. Accordingly, recent studies described a stimulation of L-type calcium channel currents due to phosphorylation by PKC in the insulin-secreting cell lines HIT-T15 and RINm5F (42, 46).

In conclusion, the present study provides the first detailed description of a $Ca_V1.3$ (L-type α_{1D}) calcium channel subunit cloned from an insulin-producing cell line. The importance of L-type channels for the exocytotic process has been stressed by several authors (5, 54). It is therefore interesting that the neuroendocrine $Ca_V1.3$ and the cardiac $Ca_V1.2a$ L-type channel subtypes, which are often coexpressed, as in insulin-secreting cells (19, 20), display significant differences with respect to specific biophysical properties. Differences in the kinetics of channel activation and inactivation suggest that the two channels may have different roles during depolarization-induced calcium influx in β-cells and consequently in insulin secretion. Most interestingly, this $Ca_V1.3$ isoform is stimulated by GPCRs in a protein kinase-dependent manner.

MATERIALS AND METHODS

Chemicals

DAMGO was purchased from RBI (Natick, MA); H7 [(±)-1-(5-isoquinolinesulfonyl)-2-methylpiperazine, 2 HCl] was from Tocris Cookson (Bristol, U.K.); and Rp-cAMPS was obtained from Calbiochem (Bad Soden, Germany). Stocks of those substances were prepared using double distilled water and stored at −20 C. The dihydropyridine (+)isradipine (R(+)-enantiomer of PN200–110) was a kind gift from Sandoz Pharmaceuticals Corp. (Basle, Switzerland). The stock solution of this substance was prepared with dimethylsulfoxide (DMSO). Collagenase type 1A and wortmannin were from Sigma-Aldrich Corp. (Deisenhofen, Germany). Wortmannin was stored in DMSO in the dark at −20 C. The calcium chelators BAPTA and the membrane permeable derivative BAPTA-AM were dissolved in a Tris-containing buffer (pH 7.2) or in DMSO and stored under N_2, respectively. Phorbol-12-myristate-13-acetate (PMA) and bisindolylmalimide I [3-(*N*-[dimethylamino] propyl-3-indolyl)-4-(3-indolyl) maleimide] were from Sigma (St. Louis, MO), and the stock solutions were prepared with DMSO. All other chemicals were of highest purity available.

Expression Plasmids and Oocyte Preparation

The identity of the $Ca_V1.3$ clone was verified by sequencing.[1] After the addition of an artificial nucleotide sequence that was constructed to optimize translation, the coding sequence started at position 9 of the original amino acid sequence (19). No other differences were found except amino acid positions

[1] The nucleotide sequence data have been submitted to the EMBL Nucleotide Sequence Database under accession number AJ311617.

427 and 428 of the original amino acid sequence where we found triplets coding for lysine and glutamine instead of asparagine and glutamate, respectively. Capped cRNA transcripts encoding $Ca_V1.3$ [*Xho*I-linearized/T7 RNA polymerase (19)], $Ca_V1.2a$ [*Kpn*I/SP6 (10)], $Ca_V2.2$ [*Sal*I/SP6 (13)], and $\alpha_2\delta$-1, termed $\alpha_2\delta$ [*Sal*I/SP6 (10)], β_3 [*Not*I/T7 (55)] calcium channel subunits as well as the μ-opioid receptor [Kas I/T7 (56)] were synthesized from the respective cDNAs using the mMessage mMachine *in vitro* transcription kit (Ambion, Inc. Austin, TX). Stage V–VI oocytes were surgically removed from adult female *Xenopus laevis* toads (African *Xenopus* Facility, Knysa, Republic of South Africa) anesthetized with 3-aminobenzoic acid ethyl ester (0.1% wt/vol) according to protocols approved by state and institutional regulations. The incision was sutured immediately after removal of the oocytes and the animals returned to the tank after recovery from surgery. They were then allowed to recover for at least 6 months before being reused as oocyte donors. Follicular cell-free oocytes were obtained by enzymatic isolation using collagenase type 1A (2 mg/ml) in Ca^{2+}-free Barth's solution (in mM: NaCl, 88; KCl, 1; $NaHCO_3$, 2.4, $MgSO_4$, 0.82; HEPES, 10; pH 7.4 with NaOH) for 2 h and then stored in Ca^{2+}-containing Barth's solution (in mM: NaCl, 88; KCl, 1; $NaHCO_3$, 2.4; $MgSO_4$, 0.82; HEPES, 10; $CaCl_2$, 0.41; $Ca(NO_3)_2$, 0.33; pH 7.4 with NaOH) supplemented with 2.5 mM sodium pyruvate, 0.1% wt/vol BSA, and 100 μg/ml gentamycin at 18 C. The oocytes were allowed to recover for 24 h and then injected with the same relative proportions of the appropriate cRNAs at a concentration of 0.1 μg/μl. Using a Nanoject Oocyte Injector (Drummond Scientific Co., Broomall, PA), 50 nl of cRNA mixture were injected per oocyte. Barth's solution was renewed daily and cells were used on days 2–7 after injection, depending on the measured current amplitudes and the quality of the oocytes.

For clarity, the following synonyms were used for the respective injected subunit combinations: neuroendocrine calcium channel for $Ca_V1.3/\beta_3/\alpha_2\delta$, cardiac $Ca_V1.2a$ calcium channel for $Ca_V1.2a/\beta_3/\alpha_2\delta$, endogenous oocyte calcium channel for $\beta_3/\alpha_2\delta$, and neuronal calcium channel for $Ca_V2.2/\beta_3/\alpha_2\delta$.

Electrophysiological Recording

Two-electrode voltage-clamp currents were recorded using an Oocyte clamp OC-725A amplifier (Warner Instrument Corp., Hamden, CT). Voltage commands were generated and currents recorded using a personal computer interfaced with an TL-1 DMA Interface (Axon Instruments, Foster City, CA) to the amplifier and using the pClamp version 6 software (Axon Instruments). Microelectrodes were filled with 3 M KCl and had typical resistances of 0.5–2.5 MΩ. The bath was connected to the clamp circuit via a 3 M KCl-agar bridge. The bath solution contained in mM: $Ba(OH)_2$, 35, NaOH, 50; HEPES, 10; pH 7.4 with methanesulfonic acid. Ba^{2+} was used as the charge carrier in all calcium channel experiments. For experiments on calcium-dependent chloride currents, modified frog Ringer (in mM: NaCl, 90; KCl, 2.5; $CaCl_2$, 1.8; HEPES, 10; pH 7.4 with NaOH) was used. Throughout all experiments, including drug applications, the bath was continuously perfused with solution at a rate of 2 ml/min. Oocytes were clamped at a holding potential of -60 mV, in the case of the steady-state inactivation experiments it was -80 mV. Only those recordings were used where currents could be adequately voltage clamped. For all experiments conducted with $Ca_V1.3$, $Ca_V1.2a$, or $Ca_V2.2$-calcium channels, at least five control oocytes injected with a corresponding amount of $\alpha_2\delta$ and β_3 cRNA were measured on the same day. Only those oocyte batches were used for analysis for which the resulting endogenous calcium current in control oocytes comprised less than 20% of the total inward barium current in oocytes expressing the exogenous channels. In the case of experiments where current kinetics were determined, the maximum endogenous currents were $<$20% of the total current. Only those experiments were considered for final analysis that showed inward holding currents of less than 10% of the maximum inward current and only minimal fluctuations during the course of the experiment.

Data Analysis and Presentation

Where appropriate, values are given as means $\pm$ SE. Statistical significance was evaluated by one-way ANOVA, and individual *P* values are given. The term n represents the number of oocytes tested. Curve fitting was done by a least-squares minimization method using the following equations. For I-V curves:

$$I = g(V_t - E)/\{1 + \exp[(V_{1/2} - V_t)/k]\} \quad (1)$$

where g is the maximum conductance, V_t the test potential, E the apparent reversal potential, $V_{1/2}$ the potential of half-activation, and k a slope factor. For steady-state inactivation curves,

$$I = (1 - C)/\{1 + \exp[(V_p - V_{1/2})/k] + C\} \quad (2)$$

where V_p is the prepulse potential, C a baseline, and I has inactivated by half at the prepulse potential indicated by $V_{1/2}$ with an e-fold change over k mV. For determination of channel activation from tail currents,

$$I = (1 - C)/\{1 + \exp[(V_t - V_{1/2})/k] + C \quad (3)$$

as in the preceding equation, with V_t the test potential and $V_{1/2}$ the potential of half-maximal activation. For the analysis of tail currents only well clamped oocytes were selected, and to avoid contamination by the capacity transient, values were taken 4 msec after the voltage step.

For monoexponential or biexponential fitting of inactivation during a voltage step,

$$I = A_1\exp(-t/\tau_1) + C \text{ (Eq 4) or } I = A_1\exp(-t/\tau_1) + A_2\exp(-t/\tau_2) + C \quad (5)$$

respectively, where τ is the time (t) at which the current had decreased to 1/e of its initial amplitude, A is the maximal amplitude of the component, and C is the steady-state current levels. Dose-response curves for (+)isradipine were fitted applying

$$I = 1 - f\{1/[1 + (IC_{50}/c)^n]\} \quad (6)$$

where f represents the maximal fraction of current responsive to the substance, which was calculated by subtracting the relative contribution of endogenous inward Ba^{2+} current from total inward current. The IC_{50} value is the substance concentration resulting in half-maximal current inhibition, and c is the substance concentration tested. The Hill coefficient, n, was set to 1. When normalized data were fitted, the same equations apply for I/I_{max}.

DAMGO was used to activate the μ-opioid receptor expressed after coinjection of its cRNA. The resulting effect on each current was calculated between the last data point before agonist application and the point of maximal effect. Current run-down was not taken into account.

Acknowledgments

We thank the following for generous gifts of cDNAs: Dr. L. Birnbaumer, (University of California, Los Angeles, CA), $Ca_V1.3$; Dr. F. Hofmann (Technische Universität München, Munich, Germany), $Ca_V1.2a$, β_3, $\alpha_2\delta$; Dr. Y. Fujita (Matsushita Electric Industrial Co., Seika, Japan), $Ca_V2.2$; and Dr. L. Emorine (Institut de Pharmacologie et de Biologie Structurale, Toulouse, France), μ-opioid receptor. We thank Dr. Günther Schultz for continuous support. We also thank Drs. A. Zobel, C. Canti, and A. G. Obukhov for introduction into the *Xenopus*

laevis oocyte model, as well as A. Tomschegg for technical assistance.

Received June 29, 2000. Revision received March 12, 2001. Accepted April 2, 2001.

Address requests for reprints to: Bernd Nürnberg, Abteilung für Pharmakologie und Toxikologie, Universität Ulm, Albert-Einstein Allee 11, D-89081 Ulm, Germany. E-mail: bernd.nuernberg@medizin.uni-ulm.de.

This work was supported by the Deutsche Forschungsgemeinschaft, Royal Society, and Fonds der Chemischen Industrie.

Note Added in Proof

While this paper was in press, Striessnig and coworkers (57) published biophysical and pharmacological properties of an α_{1D} subunit from cochlea inner hair cells.

REFERENCES

1. Ertel E, Campbell KP, Harpold MM, Hofmann F, Mori Y, Perez-Reyes E, Schwartz A, Snutch TP, Tanabe T, Birnbaumer L, Tsien RW, Catterall WA 2000 Nomenclature of voltage-gated calcium channels. Neuron 25:533–535
2. Iwashima Y, Pugh W, Depaoli AM, Takeda J, Seino S, Bell GI, Polonsky KS 1993 Expression of calcium channel mRNAs in rat pancreatic islets and downregulation after glucose infusion. Diabetes 42:948–55
3. Plant TD 1988 Properties and calcium-dependent inactivation of calcium currents in cultured mouse pancreatic B-cells. J Physiol (Lond) 404:731–47
4. Zhuang H, Bhattacharjee A, Hu F, Zhang M, Goswami T, Wang L, Wu S, Berggren PO, Li M 2000 Cloning of a T-type Ca^{2+} channel isoform in insulin-secreting cells. Diabetes 49:59–64
5. Ligon B, Boyd AE, Dunlap K 1998 Class A calcium channel variants in pancreatic islets and their role in insulin secretion. J Biol Chem 273:13905–13911
6. Homaidan FR, Sharp GW, Nowak LM 1991 Galanin inhibits a dihydropyridine-sensitive Ca^{2+} current in the RINm5f cell line. Proc Natl Acad Sci USA 88:8744–8748
7. Degtiar VE, Harhammer R, Nürnberg B 1997 Receptors couple to L-type calcium channels via distinct G_o proteins in rat neuroendocrine cell lines. J Physiol (Lond) 502:321–333
8. Pollo A, Lovallo M, Biancardi E, Sher E, Socci C, Carbone E 1993 Sensitivity to dihydropyridines, ω-conotoxin and noradrenaline reveals multiple high-voltage-activated Ca^{2+} channels in rat insulinoma and human pancreatic β-cells. Pflugers Arch 423:462–471
9. Bourinet E, Soong TW, Stea A, Snutch TP 1996 Determinants of the G protein-dependent opioid modulation of neuronal calcium channels. Proc Natl Acad Sci USA 93: 1486–1491
10. Singer D, Biel M, Lotan I, Flockerzi V, Hofmann F, Dascal N 1991 The roles of the subunits in the function of the calcium channel. Science 253:1553–1557
11. Bourinet E, Zamponi GW, Stea A, Soong TW, Lewis BA, Jones LP, Yue DT, Snutch TP 1996 The α_{1E} calcium channel exhibits permeation properties similar to low-voltage-activated calcium channels. J Neurosci 16: 4983–4993
12. Canti C, Page KM, Stephens GJ, Dolphin AC 1999 Identification of residues in the N terminus of α1B critical for inhibition of the voltage-dependent calcium channel by $G\beta\gamma$. J Neurosci 19:6855–6864
13. Fujita Y, Mynlieff M, Dirksen RT, Kim MS, Niidome T, Nakai J, Friedrich T, Iwabe N, Miyata T, Furuichi T 1993 Primary structure and functional expression of the ω-conotoxin-sensitive N-type calcium channel from rabbit brain. Neuron 10:585–598
14. Stephens GJ, Page KM, Burley JR, Berrow NS, Dolphin AC 1997 Functional expression of rat brain cloned α1E calcium channels in COS-7 cells. Pflugers Arch 433: 523–532
15. Lee JH, Daud AN, Cribbs LL, Lacerda AE, Pereverzev A, Klockner U, Schneider T, Perez-Reyes E 1999 Cloning and expression of a novel member of the low voltage-activated T-type calcium channel family. J Neurosci 19: 1912–1921
16. Cribbs LL, Gomora JC, Daud AN, Lee JH, Perez-Reyes E 2000 Molecular cloning and functional expression of $Ca_V3.1c$, a T-type calcium channel from human brain. FEBS Lett 466:54–58
17. Ihara Y, Yamada Y, Fujii Y, Gonoi T, Yano H, Yasuda K, Inagaki N, Seino Y, Seino S 1995 Molecular diversity and functional characterization of voltage-dependent calcium channels (CACN4) expressed in pancreatic β-cells. Mol Endocrinol 9:121–130
18. Williams ME, Feldman DH, McCue AF, Brenner R, Velicelebi G, Ellis SB, Harpold MM 1992 Structure and functional expression of α_1, α_2, and β subunits of a novel human neuronal calcium channel subtype. Neuron 8:71–84
19. Yaney GC, Wheeler MB, Wei X, Perez-Reyes E, Birnbaumer L, Boyd AEd, Moss LG 1992 Cloning of a novel α_1-subunit of the voltage-dependent calcium channel from the β-cell. Mol Endocrinol 6:2143–2152
20. Seino S, Chen L, Seino M, Blondel O, Takeda J, Johnson JH, Bell GI 1992 Cloning of the α1 subunit of a voltage-dependent calcium channel expressed in pancreatic β cells. Proc Natl Acad Sci USA 89:584–588
21. Birnbaumer L, Campbell KP, Catterall WA, Harpold MM, Hofmann F, Horne WA, Mori Y, Schwartz A, Snutch TP, Tanabe T 1994 The naming of voltage-gated calcium channels. Neuron 13:505–506
22. Dolphin AC 1999 L-type calcium channel modulation. Adv Second Messenger Phosphoprotein Res 33:153–77
23. Hofmann F, Lacinova L, Klugbauer N 1999 Voltage-dependent calcium channels: from structure to function. Rev Physiol Biochem Pharmacol 139:33–87
24. Plant TD, Schirra C, Katz E, Uchitel OD, Konnerth A 1998 Single-cell RT-PCR and functional characterization of Ca^{2+} channels in motoneurons of the rat facial nucleus. J Neurosci 18:9573–84
25. Hell JW, Westenbroek RE, Warner C, Ahlijanian MK, Prystay W, Gilbert MM, Snutch TP, Catterall WA 1993 Identification and differential subcellular localization of the neuronal class C and class D L-type calcium channel α1 subunits. J Cell Biol 123:949–962
26. Chik CL, Liu QY, Li B, Klein DC, Zylka M, Kim DS, Chin H, Karpinski E, Ho AK 1997 α_{1D} L-type Ca(2+)-channel currents: inhibition by a β-adrenergic agonist and pituitary adenylate cyclase-activating polypeptide (PACAP) in rat pinealocytes. J Neurochem 68:1078–1087
27. Yang SN, Larsson O, Branstrom R, Bertorello AM, Leibiger B, Leibiger IB, Moede T, Kohler M, Meister B, Berggren PO 1999 Syntaxin 1 interacts with the L_D subtype of voltage-gated Ca^{2+} channels in pancreatic β cells. Proc Natl Acad Sci USA 96:10164–10169
28. Horvath A, Szabadkai G, Varnai P, Aranyi T, Wollheim CB, Spat A, Enyedi P 1998 Voltage dependent calcium channels in adrenal glomerulosa cells and in insulin producing cells. Cell Calcium 23:33–42
29. Lacerda AE, Perez-Reyes E, Wei X, Castellano A, Brown AM 1994 T-type and N-type calcium channels of *Xeno-*

pus oocytes: evidence for specific interactions with β subunits. Biophys J 66:1833–1843
30. De Waard M, Campbell KP 1995 Subunit regulation of the neuronal α_{1A} Ca^{2+} channel expressed in *Xenopus* oocytes. J Physiol (Lond) 485:619–634
31. Wang Z, Grabner M, Berjukow S, Savchenko A, Glossmann H, Hering S 1995 Chimeric L-type Ca^{2+} channels expressed in *Xenopus laevis* oocytes reveal role of repeats III and IV in activation gating. J Physiol (Lond) 486:131–137
32. Bourinet E, Fournier F, Nargeot J, Charnet P 1992 Endogenous *Xenopus*-oocyte Ca-channels are regulated by protein kinases A and C. FEBS Lett 299:5–9
33. Gollasch M, Hescheler J, Spicher K, Klinz FJ, Schultz G, Rosenthal W 1991 Inhibition of Ca^{2+} channels via α_2-adrenergic and muscarinic receptors in pheochromocytoma (PC-12) cells. Am J Physiol 260:C1282–C1289
34. Ammala C, Berggren PO, Bokvist K, Rorsman P 1992 Inhibition of L-type calcium channels by internal GTP [γS] in mouse pancreatic β cells. Pflugers Arch 420:72–77
35. Qin N, Platano D, Olcese R, Stefani E, Birnbaumer L 1997 Direct interaction of G$\beta\gamma$ with a C-terminal G$\beta\gamma$-binding domain of the Ca^{2+} channel α1 subunit is responsible for channel inhibition by G protein-coupled receptors. Proc Natl Acad Sci USA 94:8866–8871
36. Ikeda SR 1996 Voltage-dependent modulation of N-type calcium channels by G-protein $\beta\gamma$ subunits. Nature 380: 255–258
37. Gaibelet G, Meilhoc E, Riond J, Saves I, Exner T, Liaubet L, Nürnberg B, Masson JM, Emorine LJ 1999 Nonselective coupling of the human μ-opioid receptor to multiple inhibitory G-protein isoforms. Eur J Biochem 261: 517–523
38. Ikeda SR, Dunlap K 1999 Voltage-dependent modulation of N-type calcium channels: role of G protein subunits. Adv Second Messenger Phosphoprotein Res 33: 131–151
39. Dolphin AC 1998 Mechanisms of modulation of voltage-dependent calcium channels by G proteins. J Physiol (Lond) 506:3–11
40. Zamponi GW, Bourinet E, Nelson D, Nargeot J, Snutch TP 1997 Crosstalk between G proteins and protein kinase C mediated by the calcium channel α_1 subunit. Nature 385:442–446
41. Gollasch M, Haller H, Schultz G, Hescheler J 1991 Thyrotropin-releasing hormone induces opposite effects on Ca^{2+} channel currents in pituitary cells by two pathways. Proc Natl Acad Sci USA 88:10262–10266
42. Love JA, Richards NW, Owyang C, Dawson DC 1998 Muscarinic modulation of voltage-dependent Ca^{2+} channels in insulin-secreting HIT-T15 cells. Am J Physiol 274:G397–405
43. Hidaka H, Inagaki M, Kawamoto S, Sasaki Y 1984 Isoquinolinesulfonamides, novel and potent inhibitors of cyclic nucleotide dependent protein kinase and protein kinase C. Biochemistry 23:5036–5041
44. Ludwig A, Flockerzi V, Hofmann F 1997 Regional expression and cellular localization of the α1 and β subunit of high voltage-activated calcium channels in rat brain. J Neurosci 17:1339–1349
45. Hopkins WF, Satin LS, Cook DL 1991 Inactivation kinetics and pharmacology distinguish two calcium currents in mouse pancreatic B-cells. J Membr Biol 119:229–239
46. Platano D, Pollo A, Carbone E, Aicardi G 1996 Up-regulation of L- and non-L, non-N-type Ca^{2+} channels by basal and stimulated protein kinase C activation in insulin-secreting RINm5F cells. FEBS Lett 391:189–194
47. Schmidt A, Hescheler J, Offermanns S, Spicher K, Hinsch KD, Klinz FJ, Codina J, Birnbaumer L, Gausepohl H, Frank R, Schultz G, Rosenthal W 1991 Involvement of pertussis toxin-sensitive G-proteins in the hormonal inhibition of dihydropyridine-sensitive Ca^{2+} currents in an insulin-secreting cell line (RINm5F). J Biol Chem 266: 18025–18033
48. Bell DC, Butcher AJ, Berrow NS, Page KM, Brust PF, Nesterova A, Stauderman KA, Seabrook GR, Nürnberg B, Dolphin AC 2001 Biophysical properties, pharmacology, and modulation of human, neuronal L-type (α_{1D}, $Ca_V1.3$) voltage-dependent calcium currents. J Neurophysiol 85:816–827
49. Davies SP, Reddy H, Caivano M, Cohen P 2000 Specificity and mechanism of action of some commonly used protein kinase inhibitors. Biochem J 351:95–105
50. Viard P, Exner T, Maier U, Mironneau J, Nürnberg B, Macrez N 1999 G$\beta\gamma$ dimers stimulate vascular L-type Ca^{2+} channels via phosphoinositide 3-kinase. FASEB J 13:685–694
51. Maier U, Babich A, Macrez N, Leopoldt D, Gierschik P, Illenberger D, Nürnberg B 2000 G$\beta_5\gamma_2$ is a highly selective activator of phospholipid-dependent enzymes. J Biol Chem 275:13746–13754
52. Exton JH 1996 Regulation of phosphoinositide phospholipases by hormones, neurotransmitters, and other agonists linked to G proteins. Annu Rev Pharmacol Toxicol 36:481–509
53. Stehno-Bittel L, Krapivinsky G, Krapivinsky L, Perez-Terzic C, Clapham DE 1995 The G protein β γ subunit transduces the muscarinic receptor signal for Ca^{2+} release in *Xenopus* oocytes. J Biol Chem 270: 30068–30074
54. Bokvist K, Eliasson L, Ämmälä C, Renström E, Rorsman P 1995 Co-localization of L-type Ca^{2+} channels and insulin-containing secretory granules and its significance for the initiation of exocytosis in mouse pancreatic B-cells. EMBO J 14:50–57
55. Hullin R, Singer-Lahat D, Freichel M, Biel M, Dascal N, Hofmann F, Flockerzi V 1992 Calcium channel β subunit heterogeneity: functional expression of cloned cDNA from heart, aorta and brain. EMBO J 11:885–890
56. Gaibelet G, Capeyrou R, Dietrich G, Emorine LJ 1997 Identification in the μ-opioid receptor of cysteine residues responsible for inactivation of ligand binding by thiol alkylating and reducing agents. FEBS Lett 408: 135–140
57. Koschak A, Reimer D, Huber IG, Grabner M, Glossman H, Engel J, Striessnig J 2001 α_{1D} (Cav1.3) subunits can form L-type Ca^{2+} channels activating at negative voltages. J Biol Chem M101469200 (papers in press online)